



**HAL**  
open science

## A snapshot of electrified nanodroplets undergoing Coulomb fission

S. Arscott, Cédric Descatoire, Lionel Buchaillot, Alison Ashcroft

► **To cite this version:**

S. Arscott, Cédric Descatoire, Lionel Buchaillot, Alison Ashcroft. A snapshot of electrified nanodroplets undergoing Coulomb fission. *Applied Physics Letters*, 2012, 100 (7), pp.074103. 10.1063/1.3684979 . hal-02345724

**HAL Id: hal-02345724**

**<https://hal.science/hal-02345724v1>**

Submitted on 27 May 2022

**HAL** is a multi-disciplinary open access archive for the deposit and dissemination of scientific research documents, whether they are published or not. The documents may come from teaching and research institutions in France or abroad, or from public or private research centers.

L'archive ouverte pluridisciplinaire **HAL**, est destinée au dépôt et à la diffusion de documents scientifiques de niveau recherche, publiés ou non, émanant des établissements d'enseignement et de recherche français ou étrangers, des laboratoires publics ou privés.

# A snapshot of electrified nanodroplets undergoing Coulomb fission

Cite as: Appl. Phys. Lett. **100**, 074103 (2012); <https://doi.org/10.1063/1.3684979>

Submitted: 20 September 2011 • Accepted: 26 January 2012 • Published Online: 14 February 2012

Steve Arscott, Cédric Descatoire, Lionel Buchaillot, et al.



View Online



Export Citation

## ARTICLES YOU MAY BE INTERESTED IN

### Electrospraying from nanofluidic capillary slot

Applied Physics Letters **87**, 134101 (2005); <https://doi.org/10.1063/1.2058223>

### Charge and fission of droplets in electrostatic sprays

Physics of Fluids **6**, 404 (1994); <https://doi.org/10.1063/1.868037>

### Effect of viscosity ratio on the dynamic response of droplet deformation under a steady electric field

Physics of Fluids **32**, 053301 (2020); <https://doi.org/10.1063/5.0003449>

Lock-in Amplifiers  
up to 600 MHz



Zurich  
Instruments



## A snapshot of electrified nanodroplets undergoing Coulomb fission

Steve Arscott,<sup>1,a)</sup> Cédric Descatoire,<sup>1</sup> Lionel Buchaillet,<sup>1</sup> and Alison E. Ashcroft<sup>2</sup>

<sup>1</sup>*Institut d'Electronique, de Microélectronique et de Nanotechnologie (IEMN), CNRS UMR-8520, University of Lille, Avenue Poincaré, Cite Scientifique, Villeneuve d'Ascq 59652, France*

<sup>2</sup>*Astbury Centre for Structural Molecular Biology, University of Leeds, Leeds LS2 9JT, United Kingdom*

(Received 20 September 2011; accepted 26 January 2012; published online 14 February 2012)

We investigate the size distribution of electrically charged nanodroplets using atomic force microscopy (AFM). The droplets were generated using nano- and micro-scale silicon tips. A brief voltage pulse results in a “snapshot” of charged nanodroplets on a Cr surface. AFM of the traces left by the nanodroplets revealed that certain droplet diameters are favored suggesting droplet fission due to Rayleigh instability at nanometer length scales. The most occurring droplet diameters are 85.9(4.1) nm and 167.1 nm (9.7 nm) for nano- and micro-scale tips, respectively. © 2012 American Institute of Physics. [doi:10.1063/1.3684979]

In 1882, Lord Rayleigh<sup>1</sup> predicted that a charged droplet will be unstable if the electrical charge  $q$  it carries exceeds a value given by

$$q > \sqrt{8\pi^2\gamma\epsilon_0 d^3}, \quad (1)$$

where  $d$  is the droplet diameter,  $\gamma$  is the surface tension, and  $\epsilon_0$  is the permittivity of free space. Coulomb fission, due to this instability, has recently been observed for micrometer-sized droplets.<sup>2</sup> We demonstrate, here, a technique to analyze a “snapshot” of charged nanometer-sized droplets under Rayleigh instability. A nanometer-scale silicon tip is used to deposit<sup>3</sup> nanodroplets onto a chromium (200 nm) coated silicon wafer. Atomic force microscopy (AFM) of the traces left by the nanodroplets suggests Coulomb fission occurring at these length scales.

The experimental set-up is shown in Fig. 1(a). The tips are composed of two triangular cantilevers attached to a silicon support chip. The two cantilevers define a micrometer capillary slot leading up to a nanometer scale capillary slot at the apex of the tip [Fig. 1(b)]. The tip apex has a nanometer scale channel which was defined using focused ion beam milling.<sup>4</sup> A nanometer-scale tip was tested which had a channel width of 350 nm ( $\pm 10$  nm). As a comparison, a micrometer-scale tip<sup>5</sup> was also tested which had channel width of 1  $\mu\text{m}$  ( $\pm 0.1 \mu\text{m}$ ) [Fig. 1(c)]. The tip is brought into proximity to the Cr coated Si wafer using an  $xyz$  positioning stage; the tip-to-plane distance was set to  $\sim 100 \mu\text{m}$ . The tip is loaded with the liquid ( $v \sim 5 \mu\text{l}$ ) composed of a 75:25  $v/v$  deionized water ( $\rho > 10 \text{ M}\Omega \text{ cm}$ )-methanol mixture with nitric acid ( $c = 0.001 \text{ M}$ ). A gold wire (diameter = 250  $\mu\text{m}$ ) is inserted into the droplet to serve as an electrode. A voltage pulse (0–200 V for 10 ms) is applied to the liquid which causes electro spraying at the apex of the tip.<sup>6</sup> For a point-to-plane electric field distribution,<sup>7</sup> the field decreases rapidly in a non-linear fashion in the axial direction away from the point. During the experiments, the electric field at the tip was sufficient to produce electro spraying<sup>6</sup> and decreases rapidly to  $< 4 \text{ kV cm}^{-1}$  at the Cr surface. Arcing behaviour<sup>8</sup> was

not observed in the current-voltage sweeps but rather a characteristic electro spray current-voltage.<sup>9</sup> Charged droplets are attracted towards the Cr coated Si wafer which is grounded [Fig. 1(a)]. The time-of-flight of the droplets is calculated to be of the order of tens of microseconds by numerically resolving a point-to-plane electric field model.<sup>7</sup> Break-up of a cone-jet<sup>10,11</sup> results in the formation of the electro spray plume as the charged droplets repel each other. During the time-of-flight, the charged droplets which exceed the Rayleigh criterion<sup>1</sup> will undergo Coulomb fission which has been the subject of much research.<sup>3</sup> Characterizing the distribution of micrometer-sized charged droplets can be done using optical means.<sup>2,3,12,13</sup> In contrast, the method

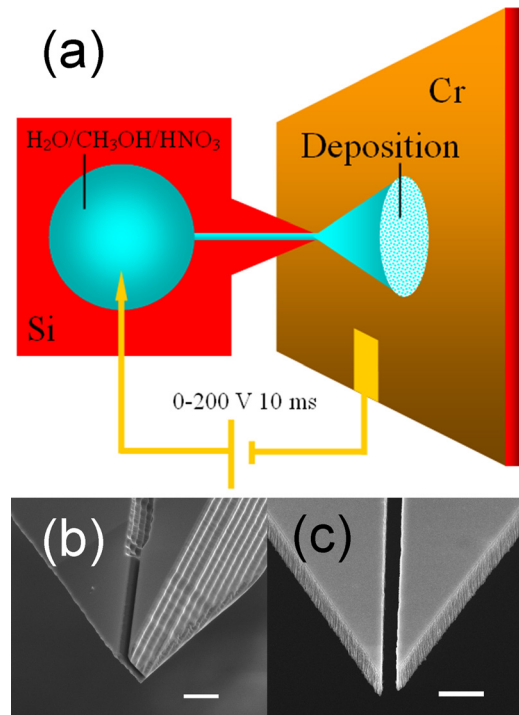


FIG. 1. (Color online) Deposition of nanodroplets onto a metal screen. (a) Experimental set-up showing the nano/micro-machined silicon tip, the liquid (water/methanol/nitric acid), the Cr coated Si wafer, and application of a voltage pulse (0–200 V) between the liquid and the wafer. (b) An SEM image of the nano-scale tip (scale bar = 1  $\mu\text{m}$ ). (c) An SEM image of the micro-scale tip (scale bar = 2  $\mu\text{m}$ ).

<sup>a)</sup>Electronic mail: steve.arscott@iemn.univ-lille1.fr.

demonstrated, here, can characterize *individual nanodroplets* according to their size and occurrence. Literature is scarce concerning imaging individual charged nanodroplets originating from an electro spray; scanning electron microscopy and near-field microscopy techniques have been used to characterize nanodroplets deposited onto surfaces.<sup>14–18</sup> We use near-field microscopy techniques, here, to characterize the traces left by charged nanodroplets after evaporation.

Fig. 2(a) shows an image obtained by tapping-mode AFM imaging (Bioscope, Veeco, USA) of the Cr surface following experiments with the nanotip. The traces are typically composed of a central area  $\sim 10\ \mu\text{m}$  in diameter surrounded by a halo<sup>7</sup> of much smaller sub-micrometer diameter satellite “spots”<sup>7</sup> characteristic of electrostatic repulsion.<sup>13</sup> Each satellite spot [Fig. 2(b)] has a central “bump” characteristic of a non-volatile residue<sup>14</sup> possibly due to impurities (rainbow colors in Fig. 2(b), surrounded by a flat “plateau” region [brown in Fig. 2(b)] not reported in the previous studies.<sup>15–19</sup>

The trace diameters are  $\sim 50\ \mu\text{m}$  (inset of Fig. 2(c) which shows that smaller droplets are found towards the periphery of the trace), implying an electro spray plume angle of around  $30^\circ$ ; this is consistent with previous observations.<sup>7,13</sup>

By analyzing these images we can produce Fig. 2(c) which shows a plot of the normalized spot number ( $n/N_t$ ;  $N_t$  = total number of spots) versus spot width  $w$  for two tips. It is apparent from Fig. 2(c) that certain spot diameters are favored and occur in bunches (see steps in Fig. 2(d) indicated by black arrows). By statistically binning the experimental data presented in Fig. 2(c) using a suitable class interval, we can produce histograms for the spot width  $w$  versus droplet occurrence  $N_{\text{exp}}$ ; the result of this is shown in Figs. 2(e) and 2(f). To explain these results let us recall that a charged droplet distribution has few large droplets (the fissility<sup>1</sup>  $X = q^2/8\pi^2\epsilon_0\gamma d^3$  is large) and few small droplets ( $X$  is small) but is composed of many droplets of distinct radii in the vicinity of  $X \sim 1$ ; the distributions in Figs. 2(e) and 2(f) are indicative

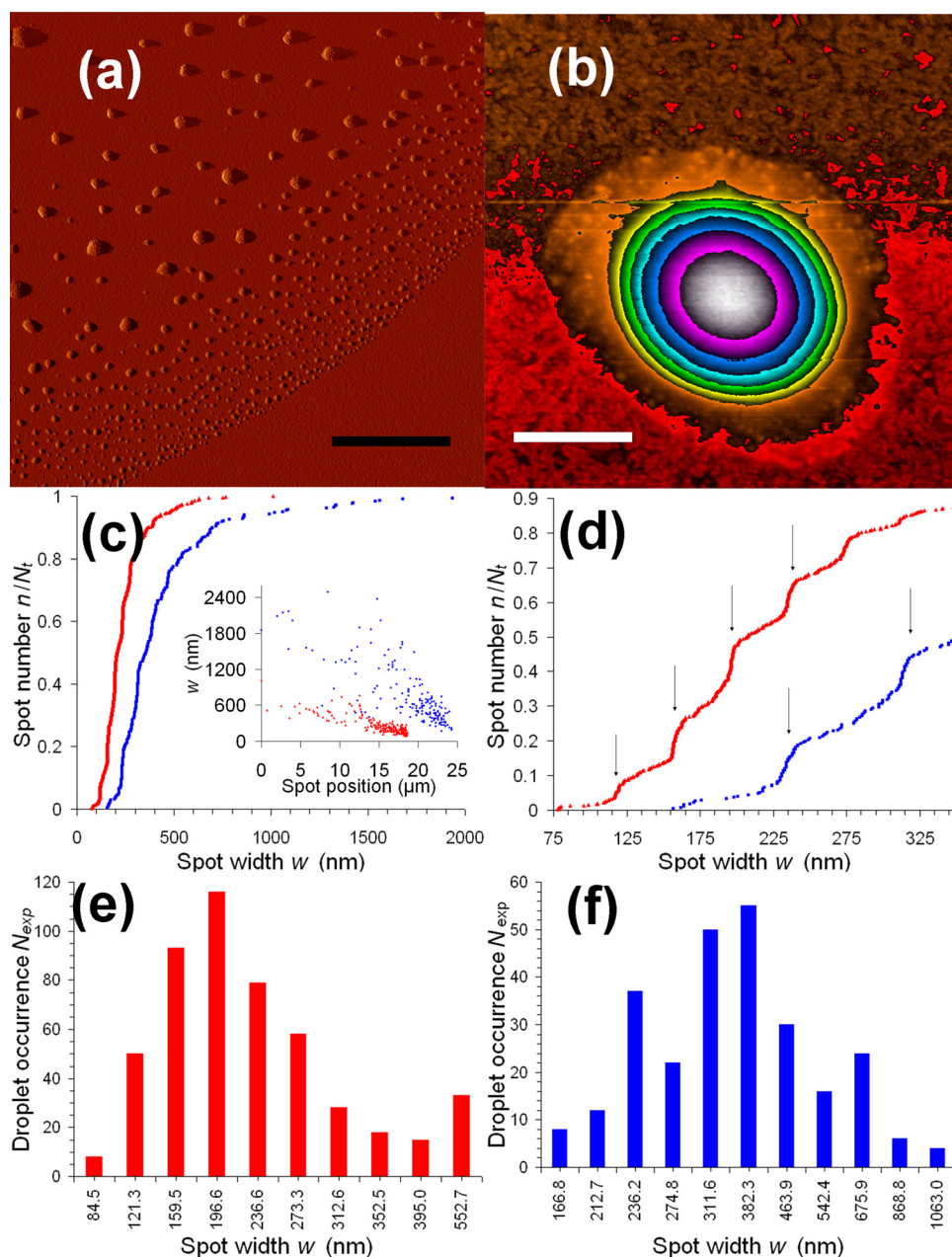


FIG. 2. (Color online) Snapshot of nanodroplets. (a) AFM imaging following experiments using the nano-scale tip (scale bar =  $5\ \mu\text{m}$ ). (b) Zoom on a single spot (scale bar =  $500\ \text{nm}$ ). (c) Plots of the spot number  $n$  divided by total number of spots  $N_t$  versus the spot width  $w$  obtained using the nanotip (red triangles) and the microtip (blue squares) [inset shows spot width versus spot position in trace]. (d) zoom of  $w$  versus  $n/N_t$  reveals steps in the plots (black arrows). (e) Histogram of spot width distribution using the nano-scale tip (red bars). (f) Histogram of spot width distribution using the micro-scale tip (blue bars).

of this. Traces produced using the nanotip result in a minimum spot width variation of 77.9–1101 nm, whereas microtip results in 157–2578 nm.

In order to interpret our observations, Fig. 3 illustrates a charged droplet impinging on the metal surface where local oxidation<sup>20</sup> and desposition<sup>21</sup> can occur; the result of this is a modification of the surface resulting in a spot having a diameter  $w$ . As a first approximation, we can relate  $w$  to the original impinging droplet diameter  $d$  by using a model based on the macroscopic wetting contact angle  $\theta$  of the water-methanol-nitric acid mixture on a Cr surface; although it should be noted that a more accurate model would require nanodroplet wetting<sup>15</sup> and charge effects to be taken into account. However, in a first approximation, which ignores droplet deformation due to electric fields,<sup>22</sup> as  $d = \alpha w$  where  $\alpha^3 = (2 - 3\cos\theta + \cos^3\theta)/4\sin^3\theta$  and  $\theta$  was measured to be  $24.7 (\pm 2)^\circ$  using a contact angle meter (Kruss, Germany), we determine the parameter  $\alpha$  to be 0.437. This enables a calculation of the experimental droplet diameters ( $d_{\text{exp}}$ ) shown in Tables I and II. The experimental droplet diameters  $d_{\text{exp}}$  are mean values calculated over the class interval. The observations can be analyzed in terms of (i) droplet size distribution and (ii) volume flow rate.

First, in terms of the droplet size distribution although electrically charged droplet distribution populations are known to be highly complex,<sup>23</sup> a simple fission model based on droplet volume halving can be compared with the experimental results. This simplistic model can check for a signature of droplet break-up at these length scales, presumably due to Rayleigh instability.<sup>1</sup> By choosing an highly occurring droplet diameter  $d_n$  (underlined bold values in Tables I and II) observed in the experimental AFM data, we can calculate a set of droplet diameters based on simple volume halving:  $V_{n+1} = V_n/2 \Rightarrow d_{n+1} = d_n/\sqrt[3]{2}$ ; these calculated droplet diameters  $d_{\text{cal}}$  are shown in Tables I and II along with the experimental droplet diameters  $d_{\text{exp}}$ . First, the nanotip results in smaller droplets than the microtip). Second, droplet splitting (by halving) is clear from the results both for the nanotip and the microtip. Third, there appears to be two sets of droplet halving happening (single star and double star values for

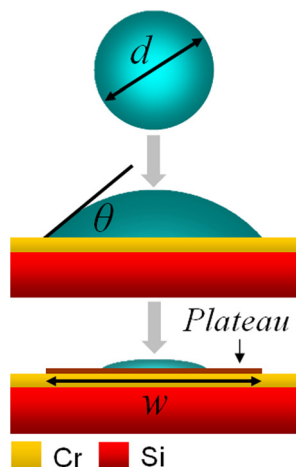


FIG. 3. (Color online) Spot width  $w$  and original droplet diameter  $d$ : schematic diagram of a droplet impinging a surface having a wetting contact angle of  $\theta$ .

TABLE I. Experimental ( $N_{\text{exp}}$  and  $d_{\text{exp}}$ ) and modeling ( $d_{\text{cal}}$ ) results for the nano-scale tip;  $d_{\text{exp}}$  corresponds to the average experimental original droplet diameter is calculated from  $w_{\text{exp}}$  (see Figure 3), and the droplet occurrence  $N_{\text{exp}}$  is the number of spots in the given spot width interval. Droplet diameters corresponding to the  $d_{n+1} = d_n/\sqrt[3]{2}$  model are shown starting from the initial bold values. Standard deviations are shown in brackets. Asterisks correspond to related droplet. Asterisks correspond to related droplet.

| $N_{\text{exp}}$ | $d_{\text{exp}}$ (nm) | $d_{\text{cal}}$ (nm) |
|------------------|-----------------------|-----------------------|
| 8                | 36.9(3.4)             | 34.1*                 |
| 50               | 53.0(3.4)             | 54.1*                 |
| 93               | 69.7(3.7)             | 68.2*                 |
| 116              | 85.9(4.1)             | <b>85.9*</b>          |
| 79               | 103.4(3.3)            | 108.2*                |
| 58               | 119.4(3.5)            | <b>119.4**</b>        |
| 28               | 136.6(3.7)            | 136.4*                |
| 18               | 154.0(4.1)            | 150.5**               |
| 15               | 172.6(2.6)            | 171.8*                |
| 33               | 241.5(51.3)           | 238.9**               |

$d_{\text{cal}}$ ) which is clear from the simple volume halving model. Two droplet sizes in Tables I and II have large standard deviations due to few data. One can presume that the results indicate a signature of Coulomb fission and gives evidence for nanodroplet splitting due to Rayleigh instability at these length scales, although a full understanding of the droplet distribution population requires more complex models.<sup>23</sup>

By making the assumption that the most occurring droplet diameters have  $X = 1$ , we can calculate the number of unit charges to be 902 droplet<sup>-1</sup> ( $6.22 \times 10^{-3} \text{ C m}^{-2}$ ) and 2446 droplet<sup>-1</sup> ( $4.46 \times 10^{-3} \text{ C m}^{-2}$ ) for the nano- and microtip, respectively. A volume flow rate  $Q$  can be determined from the measurements. The measurement sector angle  $\psi$  for the nanotip was equal to  $31^\circ$  (corresponding to 498 spots in this AFM image or  $\sim 5700$  spots in the total trace), whereas  $\psi$  for the microtip was  $25^\circ$  (corresponding to 276 spots in this AFM image or  $\sim 3900$  spots in the total trace).  $Q$  can be calculated by summing all droplet volumes in the AFM trace and multiplying by a factor which takes into account the measurement sector  $\psi$  of the total trace. In this way, we determine  $Q$  to be equal to  $0.86(\pm 0.1) \text{ nl min}^{-1}$  (nanotip) and  $3.72(\pm 0.3) \text{ nl min}^{-1}$  (microtip). By using the physical properties of the water-methanol-nitric acid mixture: surface tension  $\gamma$  ( $\sim 47 \text{ mJ m}^{-2}$ ),<sup>24</sup> density  $\rho$  ( $\sim 844 \text{ kg m}^{-3}$ ),<sup>25</sup> and conductivity  $\sigma$  ( $\sim 1.26 \mu\text{S m}^{-1}$ ); we can compare our findings, here, to

TABLE II. Experimental ( $N_{\text{exp}}$  and  $d_{\text{exp}}$ ) and modeling ( $d_{\text{cal}}$ ) results for the micro-scale tip (see Table I for explanation). Asterisks correspond to related droplet.

| $N_{\text{exp}}$ | $d_{\text{exp}}$ (nm) | $d_{\text{cal}}$ (nm) |
|------------------|-----------------------|-----------------------|
| 8                | 72.9(2.7)             | 75.6*                 |
| 12               | 92.9(4.5)             | 95.3*                 |
| 37               | 103.2(2.5)            | 105.3**               |
| 22               | 120.1(4.6)            | <b>120.1*</b>         |
| 50               | 136.2(4)              | 132.6**               |
| 55               | 167.1(9.7)            | <b>167.1**</b>        |
| 30               | 202.7(7.8)            | —                     |
| 16               | 237.0(10)             | 240.2*                |
| 24               | 295.4(209)            | 302.6*                |
| 6                | 379.7(29.2)           | 381.2*                |
| 4                | 464.5(13.5)           | 480.3*                |

validated models and experiments in the literature.<sup>3</sup> The current  $I$  was measured to be 4.5 nA (nanotip) and 9.6 nA (microtip). The scaling law<sup>26</sup>  $Q = \beta I^2 / \gamma \sigma$ , which has been rigorously verified,<sup>3</sup> here  $\beta = 4.21 \times 10^{-5}$  and  $3.98 \times 10^{-5}$  for the nano- and microtip. For varicose “Rayleigh” break-up,<sup>27,28</sup> the most likely occurring here, the droplet diameter ( $d = 2.27\pi^{-2/3} Q^{1/2} (\rho \epsilon_0 / \gamma \sigma)^{1/6}$ ) can be calculated<sup>27</sup> to be 89.6( $\pm 5.1$ ) nm and 186.4( $\pm 7.4$ ) nm for the nano- and microtips, respectively; these values are comparable with the experimental most occurring values in Tables I and II.

In conclusion, we demonstrate a method which can produce and characterize a snapshot of nanodroplets using nanofabricated silicon tips and AFM. The study provides evidence for Coulomb fission of nanodroplets. This seems the most likely explanation for our observations as the experimental results are not characteristic of arcing,<sup>8</sup> electrowetting,<sup>29</sup> droplet impact,<sup>30</sup> or evaporation.<sup>31</sup> The approach could be useful for testing existing models,<sup>3,23</sup> characterizing phenomena such as catastrophic droplet breakup.<sup>32</sup> Also, the observations have implications for nanotechnology<sup>33</sup> as the tip size is seen to determine the deposition resolution.

<sup>1</sup>Lord Rayleigh, *Philos. Mag.* **14**, 184 (1882).

<sup>2</sup>D. Duft, T. Achtzehn, R. Müller, B. A. Huber, and T. Leisner, *Nature* **421**, 128 (2003).

<sup>3</sup>A. M. Ganan-Calvo and A. M. Montanero, *Phys. Rev. E* **79**, 066305 (2009).

<sup>4</sup>S. Arscott and D. Troadec, *Nanotechnology* **16**, 2295 (2005).

<sup>5</sup>S. Arscott, S. Le Gac, and C. Rolando, *Sens. Actuators B* **106**, 741 (2005).

<sup>6</sup>S. Arscott and D. Troadec, *Appl. Phys. Lett.* **87**, 124101 (2005).

<sup>7</sup>A. M. Gañán-Calvo, J. C. Lasheras, J. Dávila, and A. Barrero, *J. Aerosol Sci.* **25**, 1121 (1994).

<sup>8</sup>R. J. Morrow, *J. Phys. D: Appl. Phys.* **30**, 3099 (1997).

<sup>9</sup>G. J. Van Berkel and F. Zhou, *Anal. Chem.* **67**, 2916 (1995).

<sup>10</sup>G. Taylor, *Proc. R. Soc. London, Ser. A* **280**, 383 (1964).

<sup>11</sup>A. M. Gañán-Calvo, *Phys. Rev. Lett.* **79**, 217 (1997).

<sup>12</sup>W. D. Bachalo and M. J. Houser, *Opt. Eng.* **23**, 583 (1984).

<sup>13</sup>A. Gomez and A. Tang, *Phys. Fluids* **6**, 404 (1994).

<sup>14</sup>U. E. A. Fittschen, N. H. Bings, S. Hauschild, S. Forster, A. F. Kiera, E. Karavani, A. Fromsdorf, and J. Thiele, *Anal. Chem.* **80**, 1967 (2008).

<sup>15</sup>A. Checco, P. Guenoun, and J. Daillant, *Phys. Rev. Lett.* **91**, 186101 (2003).

<sup>16</sup>T. C. Miller and G. J. Havrilla, *X-Ray Spectrom.* **33**, 101 (2004).

<sup>17</sup>J. Ma, G. Jing, S. Chen, and D. Yu, *J. Phys. Chem. C* **113**, 16169 (2009).

<sup>18</sup>D. Li, M. Marquez, and Y. Xia, *Chem. Phys. Lett.* **445**, 271 (2007).

<sup>19</sup>Y. C. Jung and B. Bhushan, *J. Vac. Sci. Technol. A* **26**, 777 (2008).

<sup>20</sup>J. A. Dagata, J. Schneir, H. H. Harary, C. J. Evans, M. T. Postek, and J. Bennett, *Appl. Phys. Lett.* **56**, 2001 (1990).

<sup>21</sup>O. Wilhelm, L. Madler, and S. E. Pratsinis, *J. Aerosol Sci.* **34**, 815 (2003).

<sup>22</sup>F. K. Wohlhuter and O. A. Basaran, *J. Fluid Mech.* **235**, 481 (1992).

<sup>23</sup>R. Vazquez and A. M. Gañán-Calvo, *J. Phys. A: Math. Theor.* **43**, 185501 (2010).

<sup>24</sup>G. Vaquez, E. Alvarez, and J. M. Navaza, *J. Chem. Eng. Data* **40**, 611 (1995).

<sup>25</sup>*CRC Handbook of Chemistry and Physics*, 69th ed., edited by R. C. Weast (CRC, Florida, USA, 1988).

<sup>26</sup>A. M. Gañán-Calvo, A. Barrero, and C. Pantano-Rubiño, *J. Aerosol Sci.* **24**, S19 (1993).

<sup>27</sup>A. M. Gañán-Calvo, J. Dávila, and A. Barrero, *J. Aerosol Sci.* **28**, 249 (1997).

<sup>28</sup>R. P. A. Hartman, J.-P. Borra1, D. J. Brunner, J. C. M. Marijnissen, and B. J. Scarlett, *Electrostatics* **47**, 143 (1999).

<sup>29</sup>F. Mugele and S. Herminghaus, *Appl. Phys. Lett.* **81**, 2303 (2002).

<sup>30</sup>M. Gamero-Castan, A. Torrents, L. Valdevit, and J.-G. Zheng, *Phys. Rev. Lett.* **105**, 145701 (2010).

<sup>31</sup>R. D. Deegan, O. Bakajin, T. F. Dupont, G. Huber, S. R. Nagel, and T. A. Witten, *Nature* **389**, 827 (1997).

<sup>32</sup>J. S. Raut, S. Akella, A. Kumar Singh, and V. M. Naik, *Langmuir* **25**, 4829 (2009).

<sup>33</sup>A. Jaworek and A. T. Sobczyk, *J. Electrostat.* **66**, 197 (2008).